Residual Stress via the Contour Method in Compact Tension Specimens produced via Selective Laser Melting

Authors: Bey Vrancken[a], Victoria Cain[b,c], Rob Knutsen[b], Jan Van Humbeeck[a]

[a] *Department of Materials Science, KU Leuven, Belgium*

[b] *Centre for Materials Engineering, Department of Mechanical Engineering, University of Cape Town, South Africa*

[c] *Department of Mechanical Engineering, Cape Peninsula University of Technology, South Africa*

Abstract

The complex thermal history of parts produced via Selective Laser Melting leads to a complex residual stress state. While it is generally accepted that these residual stresses are unfavorable, their exact influence on the mechanical behavior of parts produced by SLM is unknown. 2D stress mapping using the contour method shows that residual stresses have a major influence on the anisotropic behavior of Ti6Al4V produced via Selective Laser Melting. Furthermore, maximum stress values are close to the yield stress.

Keywords

Additive Manufacturing; Selective Laser Melting; Residual Stress; Contour Method; Fractography.

Main Body

In Selective Laser Melting, a high power laser locally melts successive layers of powder to produce complex shaped three-dimensional metal parts. The highly localized heat input leads to extremely large thermal gradients, which can surpass 10^7 K/s and 10^7 K/m [1]. In turn, these gradients produce a complex residual stress state inside the part. Stresses are introduced mainly by the shrinkage of the solidifying top layer, which is restricted by the previously consolidated layers. This induces tensile stresses in the top layer which are close or equal to the material yield stress [2], while the underlying previously consolidated material is compressed. Over time, as more and more layers are added on top of a specific point, this turns the original tensile stresses into compressive stresses.

The shrinkage of the top layer cannot be assumed to be planar isotropic, as this would neglect the track by track nature of the laser scanning. The stresses are on average two times larger in the direction of a scan track [3]. Shortening the individual tracks by adjusting the scan strategy to a so called island scanning strategy can greatly reduce residual stresses [2, 4-7]. By rotating the scan pattern between layers, the directional anisotropy of one layer is compensated for by the next layer, creating a more homogeneous stress distribution.

Several studies have been performed on residual stresses in additively manufactured parts. Most of these studies focused on thin walls produced via the LENS® process [8-12], as this geometry allows a quasi-2D approach and simplifies the analysis. It has been shown both through experiments and modelling that the vertical tensile stresses near the outer edges of the walls may exceed the material yield stress, causing cracks. Ding *et al.* [12] used an uncoupled thermo-mechanical model of a thin wall to predict residual stresses. The results, which were also quantitatively verified using neutron diffraction, showed that the longitudinal stresses were large compared to the transversal and normal stresses. Furthermore, the longitudinal stresses, tensile at the top surface, decreased more or less linearly moving downwards along the normal (vertical) direction. Moat *et al.* [13] used neutron diffraction and the contour method to map the stress field inside a thin wall. Results from both

methods coincided well and showed that the overall stress state in the part, while still attached to the base plate, can be described as being compressive in the center and tensile along the side and top surfaces. Rangaswamy *et al*. [14] also used neutron diffraction and the contour method on 3D solid structures produced via LENS® rather than a thin wall. The residual stresses were found to be small in the horizontal plane, but large in the vertical direction. The stress maps showed that mainly vertical stresses were present, which were compressive in the center and in tension along the outer surfaces. Krol *et al.* [15] modelled the effect of different support structures on the final residual stresses and validated the model with neutron diffraction measurements, showing that an optimal choice of support structure and preheating can lower the residual stresses. Contrary to the results of the authors above, Barbas *et al.* [16] measured compressive stresses on all outer surfaces but the top on a small 5 mm^3 CP2 Ti cube. Lipinski *et al.* [17] later used these results to explain the fatigue behavior of scaffolds produced by SLM.

Apart from the detailed investigations mentioned above, residual stress analysis of SLM has mainly been limited to qualitative or semi-quantitative analyses by measuring deformation rather than stresses, for instance via the use of cantilever or bridge shaped specimens [6, 7, 18]. Furthermore, residual stress modeling efforts for SLM face difficulties due to the small scale at which the phenomena are taking place, which drastically increases computational time. In general, of the major metal AM techniques, SLM suffers most from residual stresses. Preheating during electron beam melting and the large heat input during LENS® lower the thermal gradients in those processes, thereby limiting residual stress buildup. While authors such as Leuders *et al.* [19] have used residual stresses as an explanation for the mechanical behavior of Ti6Al4V processed via SLM, studies that combine both the mechanical properties and residual stresses are lacking.

Samples were produced on a SLM machine by Layerwise NV, Belgium [20] using Grade 5 Ti6Al4V powder with a powder particle size ranging between 5 and 50 µm. Nomenclature of ASTM Standard E399 was used in labeling the specimens described below. The XZ and ZX oriented samples were

produced individually. The XY oriented samples were produced in a stack, after which individual samples were sliced using EDM. The XY sample used in this paper came from the center of the stack, thus not from the bottom nor the top. Sample orientations are shown in Figure 1. Compact tension specimen dimensions are according to ASTM Standard E399. The notch was introduced using wire EDM.

For each orientation, one sample was used for residual stress measurements. Three samples per orientation were used for fracture toughness and another three fatigue crack growth rate (FCGR) testing. Another three FCGR samples per orientation were subjected to a stress relief heat treatment consisting of four hours at 650°C and furnace cooling.

FCGR tests were performed on an INSTRON Combined Schenck using a fixed amplitude ΔP and a frequency of 5 Hz. The length of the crack was monitored using a camera system.

A detailed review of the contour method and its application can be found elsewhere [21, 22]. In short, samples were cut using wire EDM with a brass wire 100 µm in diameter. To minimize cutting errors, the parts were clamped on both sides of the cut using a specifically designed holder, similar to the one shown in Ref. [21]. Duration of the cutting was about 15 minutes, resulting in a cut plane of 20 mm by 12,5 mm. The deformation of both cut planes was measured four times using a COORD3 coordinate measurement machine with a 3 mm diameter stylus. The accuracy and precision of the machine are 5 µm and 1 µm, respectively. Each surface was measured using a 0,4 mm point spacing, resulting in a 49 by 31 grid of 1519 data points. After averaging the four data sets for one surface, the raw data was cleaned and the data for the two opposing surfaces of one cut was averaged to remove all anti-symmetrical errors induced during wire EDM cutting. To avoid unrealistic local stress peaks due to random errors in the surface data, the data is then fitted with a quadratic spline approximation using a node spacing of 3,3 mm. One half of a compact tension sample is modelled in the commercially available ABAQUS finite element package. The spline is then evaluated at the ABAQUS node coordinates of the cut plane, and the measured deformation is applied to the model.

The ABAQUS model node spacing at the cut plane equals 0.3 mm, and the model consists of 51110 C3D8R-type elements. The normal stresses obtained are assumed equal to the stresses that would be needed to return the cut to a flat surface, i.e. the residual stresses that were released during cutting. Plasticity effects and the bulge error were not accounted for, but were minimized by secure clamping close to the cut and the use of a thin wire.

In Figure 2a, both halves of the fracture surfaces of a representative XY oriented sample after fracture toughness testing are shown. The bottom part of the shown surface consists of the notch that was made using EDM, and is not an actual part of the fracture surface. Above, a pre-crack is grown to approximately 7 mm in length using cyclic fatigue cracking, as dictated by ASTM standard E399. Afterwards, the sample is loaded statically with increasing force until fracture occurs. The pre-crack front is indicated by the red dashed line in the left fracture surface for clarity. The front is relatively straight. Additionally, Figure 2a also shows the residual stress map of the stresses perpendicular to the fracture surface. Peculiarly, the stresses are tensile in the center, balanced by compression at the top and bottom edge. The maximum stress values are well below the yield stress, which equals 1100 MPa or higher for Grade 5 Ti6Al4V produced via SLM [23]. Furthermore, the stress distribution appears to be slightly elongated in the building direction.

The fracture surface and stress plot for the XZ sample are shown in Figure 2b. As with the XY sample, stresses are low compared to the yield stress, and the stress distribution appears elongated along the building direction. Furthermore, the pre-crack front is again relatively straight. One major difference compared to the XY sample is that the stresses are compressive in the center, balanced by tensile stresses at the edges, as was expected.

The results for the ZX sample, shown in Figure 2c, are remarkable. The fracture surfaces clearly show that the pre-crack is not straight but curved, with the crack extending the furthest along the edges of the specimen. Moreover, the stress measurement revealed that large residual stresses are present, oriented along the building (vertical) direction, which is out of plane in the image. These stresses are

much larger than those in the XY and XZ sample, where the measured stresses are in the horizontal plane. This is in agreement with the previous measurements performed by Rangaswamy [14], who indicated that the vertical stresses are dominant over the horizontal stresses. The stress distribution shows compressive stresses in the center of the specimen. The zone of compressive stresses occupies the majority of the surface area and extend outwards towards the middle of the edge where the notch was made. Large tensile stresses at the other edges balance the compressive stresses. While caution is advised in using stress values at the edges when using the contour method, values close to the yield stress are measured, specifically at the left and right ends of the notch edge at the bottom.

The residual stress distributions and magnitudes provide a surprisingly clear insight in the behavior of the material during fabrication of the pre-crack and during fatigue crack growth rate (FCGR) testing. First, the pre-crack fronts of the XY and XZ sample are both relatively straight. The residual stresses inside those samples are fairly low compared to the yield stress. Moreover, at the notch where the pre-crack is initiated, the maximum and minimum stresses only differ by roughly 300 MPa. As the pre-crack grows, the residual stress distribution will be readjusted, and the difference will only decrease. This means that, when applying load to grow the pre-crack, the whole crack front will experience high tensile stresses and the crack will grow more or less uniformly. For the ZX sample, the maximum and minimum stress at the notch edge differ by more than 1 GPa. This means that one part of the crack front could be experiencing tensile stresses high enough to cause crack growth, while other parts experience almost no stress, or even compressive stresses. This will cause the crack to grow faster along the sides and leads to the curved shape of the pre-crack, visible in Figure 2c. The fracture toughness of the XY, XZ and ZX samples was equal to 28 ± 2 MPa, 23 ± 1 MPa and 16 ± 1 MPa, respectively. While these values are nowhere near those reported earlier for Ti6Al4V produced via SLM [24], they do illustrate the anisotropy. The highest value is achieved for the XY orientation, in which the stress field consists of compressive stresses near the edge. The lowest value belongs to the ZX orientation, in which the stresses reach the largest magnitude.

Second, the effect of the stresses at the crack front are also clearly visible in results obtained during FCGR testing. Samples for FCGR tests are only half as thick as fracture toughness samples, but the stress distribution is likely to be similar. While the ZX sample clearly stands out from the other two regarding magnitude of the stresses, the XY sample is distinguished by the sign of the stresses. The XZ and ZX sample both have compressive stresses in the center and tensile stresses along the edges. In the XY sample, the stresses at the notch are compressive. The stress the material experiences at the notch or crack tip will therefore be lower than the applied stress, causing the crack to grow slower. This is visible in Figure 3, where the FCGR of the as built (AB) XY sample (Figure 3a) can be compared to that of as built XZ (Figure 3b) and ZX (Figure 3c) samples. Further evidence of the influence of the residual stress on crack growth rates is found in the FCGR of stress relieved (SR) samples. In the XY sample, this relieves the compressive stresses that would slow down crack growth, and therefore, the FCGR is worse after stress relieving. On the other hand, relief of the tensile stresses in the ZX and XZ sample lowers the FCGR. Moreover, the FCGR for the three directions becomes more or less the same after stress relieving.

In conclusion, the residual stress inside Ti6Al4V CT-specimens produced via SLM is mainly oriented along the building direction. Furthermore, the influence of the residual stress on the fracture behavior during fracture toughness testing and FCGR testing is evident. The shape of the pre-crack is clearly influenced by the internal stress configuration, as is the FCGR. Consequently, the residual stresses are a major factor in the anisotropic behavior of material produced via SLM. Further corroboration of the influence of the residual stresses is found in the distinct effect of a stress relief treatment in the FCGR behavior.

Bey Vrancken thanks the Agency for Innovation by Science and Technology (IWT). Research partially funded by SBO Project grant 110070: eSHM with AM of the Agency for Innovation by Science and Technology (IWT) and from KULeuven GOA/10/12. In addition, this work is based on the research supported in part by the National Research Foundation of South Africa (NRF) for the grant

80561. The authors also acknowledge the Erasmus Mundus scholarship funded by the European Union.

"Any opinion, finding and conclusion or recommendation expressed in this material is that of the authors and the NRF does not accept any liability in this regard".

References

[1] Thijs L, Montero Sistiaga ML, Wauthle R, Xie Q, Kruth J-P, Van Humbeeck J. Acta Mater. 2013;61:4657.

[2] Mercelis P, Kruth JP. Rapid Prototyping J. 2006;12:254.

[3] Gusarov AV, Pavlov M, Smurov I. Physics Procedia 2011;12, Part A:248.

[4] Nickel AH, Barnett DM, Prinz FB. Materials Science and Engineering: A 2001;317:59.

[5] Klingbeil NW, Beuth J, Chin R, Amon C. Proceedings of the Solid Freeform Fabrication Symposium 1998:367.

[6] Zaeh M, Branner G. Production Engineering 2010;4:35.

[7] Kruth JP, Deckers J, Yasa E, Wauthle R. Proc. Inst. Mech. Eng. Part B-J. Eng. Manuf. 2012;226:980.

[8] Vasinonta A, Beuth J, Griffith ML. Journal of Manufacturing Science and Engineering 2007;129:101.

[9] Aggarangsi P, Beuth J, Griffith ML. Proceedings of the Solid Freeform Fabrication Symposium 2003:196.

[10] Zekovic S, Dwivedi R, Kovacevic R. Proceedings of the Solid Freeform Fabrication Symposium 2005:338.

[11] Pratt P, Felicelli SD, Wang L, Hubbard CR. Metallurgical and Materials Transactions A 2008;39:3155.

[12] Ding J, Colegrove P, Mehnen J, Ganguly S, Sequeira Almeida PM, Wang F, Williams S. Computational Materials Science 2011;50:3315.

[13] Moat RJ, Pinkerton AJ, Li L, Withers PJ, Preuss M. Materials Science and Engineering: A 2011;528:2288.

[14] Rangaswamy P, Griffith ML, Prime MB, Holden TM, Rogge RB, Edwards JM, Sebring RJ. Mater. Sci. Eng. A-Struct. Mater. Prop. Microstruct. Process. 2005;399:72.

[15] Krol TA, Seidel C, Schilp J, Hofmann M, Gan W, Zaeh MF. Physics Procedia 2013;41:849.

[16] Barbas A, Bonnet AS, Lipinski P, Pesci R, Dubois G. Journal of the Mechanical Behavior of Biomedical Materials 2012;9:34.

[17] Lipinski P, Barbas A, Bonnet AS. Journal of the Mechanical Behavior of Biomedical Materials 2013;28:274.

[18] Shiomi M, Osakada K, Nakamura K, Yamashita T, Abe F. CIRP Annals - Manufacturing Technology 2004;53:195.

[19] Leuders S, Thöne M, Riemer A, Niendorf T, Tröster T, Richard HA, Maier HJ. Int. J. Fatigue 2012.

[20] LayerWise N.V.: http://www.layerwise.com.

[21] Prime MB. J. Eng. Mater. Technol.-Trans. ASME 2001;123:162.

[22] Prime MB, Kastengren AL. Proceedings of the SEM Annual Conference & Exposition on Experimental and Applied Mechanics Indianapolis 2010.

[23] Vrancken B, Thijs L, Kruth J-P, Van Humbeeck J. J. Alloys Compd. 2012;541:177.

[24] Van Hooreweder B, Moens D, Boonen R, Kruth J-P, Sas P. Adv. Eng. Mater. 2012;14:92.

Figures

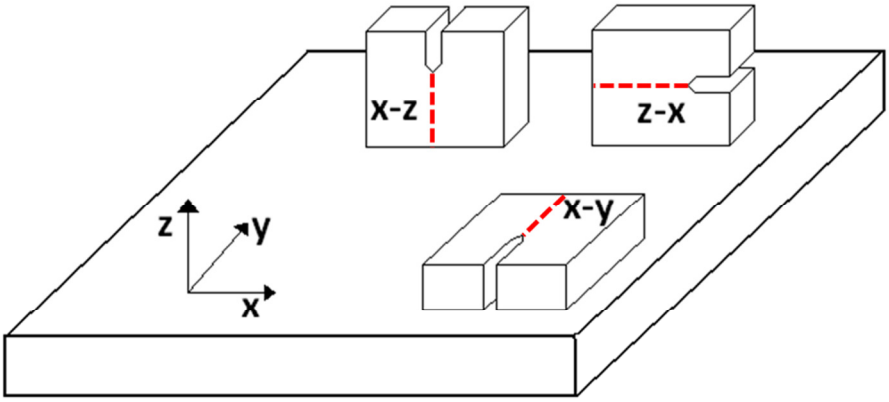

Figure 1 Sample orientations of the XZ, ZX and XY compact tension specimens. The dashed red lines indicate the direction in which the crack would normally propagate, but also indicate the plane along which the samples were cut for the contour method.

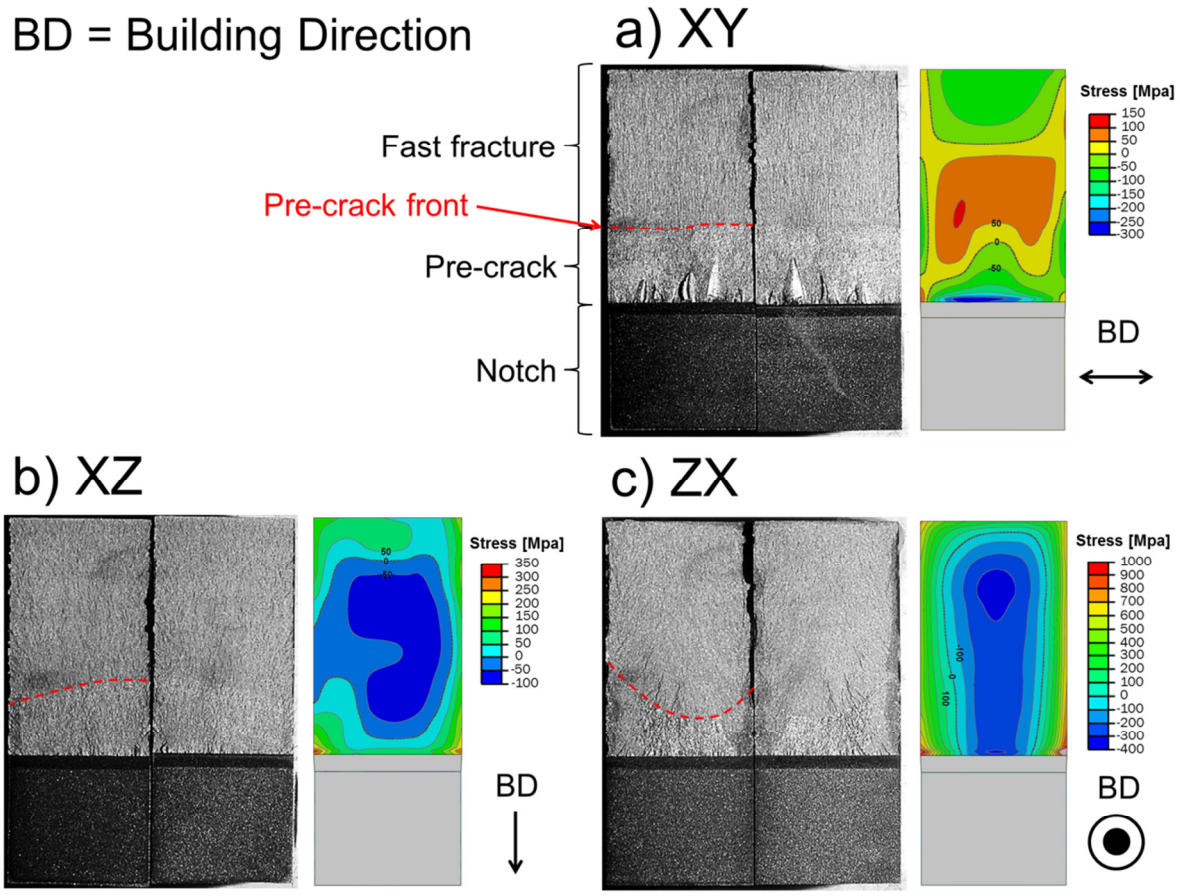

Figure 2 Representative fracture surfaces for all three orientations. The surface shown can be divided in three parts: The notch that was precut using wire EDM and is not an actual part of the fracture surface, the pre-crack and the fast fracture zone. The pre-crack front is indicated by the dashed red line. Also shown are the 2D residual stress plots obtained using the contour method, for a) the XY specimen, b) the XZ specimen and c) the ZX specimen. The stress field In the XY sample shows tension in the center, balanced by compression at the left and right edge. In the XZ and ZX sample, there are compressive stresses in the center and tensile stresses near the top and bottom edges. Notice the different scales; the stresses are much larger in the ZX specimen.

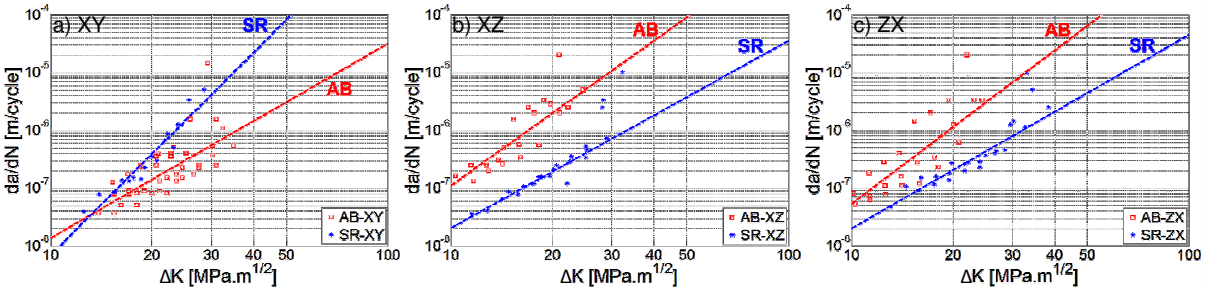

Figure 3 FCGR curves for all three orientations in the as built (AB) condition and after stress relief (SR). Note that in a), the XY orientation shows an increased FCGR after stress relieving, while the XZ and ZX orientation experience a decrease in FCGR after stress relief.